Classical transmittance and tunnelling

1991 J. Phys. A: Math. Gen. 24 2003

(http://iopscience.iop.org/0305-4470/24/9/012)

J. Phys. A: Math. Gen. **24** (1991) 2003-2012. Printed in the UK

Classical transmittance and tunnelling

J G Muga

Departamento de Física Fundamental y Experimental, Facultad de Física, Universidad de La Laguna, Tenerife, Spain

Received 3 October 1990

Abstract. A comparison is made between classical and quantum time-dependent passage through a potential barrier. The classical transmittance is defined by associating a classical ensemble to the quantum wavepacket. The conditions determining the differences between the classical and the quantum results are discussed. The classical results improve previous semiclassical methods.

1. Introduction

While the classical transmittance curve for a single particle has a step shape (it cannot pass the barrier at energies below the maximum of the barrier), the quantum transmittances for stationary scattering, i.e. for definite incident momentum, are in general smooth and allow for barrier penetration at lower energies. Accordingly, tunnelling is regarded as a purely quantum phenomenon in any quantum mechanics treatise.

However, when considering time-dependent scattering, wavepacket tunnelling, i.e. the passage through the barrier at incident *average energy* (expectation value) lower than the barrier, admits a classical explanation. It is possible, with the restrictions explained later, to reproduce with high accuracy the quantum transmittance curves even below threshold (see figure 1(a) and figure 1(b)) by associating to the wavepacket a classical ensemble in phase space rather than a single particle. We shall derive a simple formula allowing us to estimate the transmittance classically by evaluating the fraction of initial ensemble points with energy above the maximum of the barrier for initial Gaussian wavepackets. We shall also discuss the conditions favouring the differences between the classical and the quantum results.

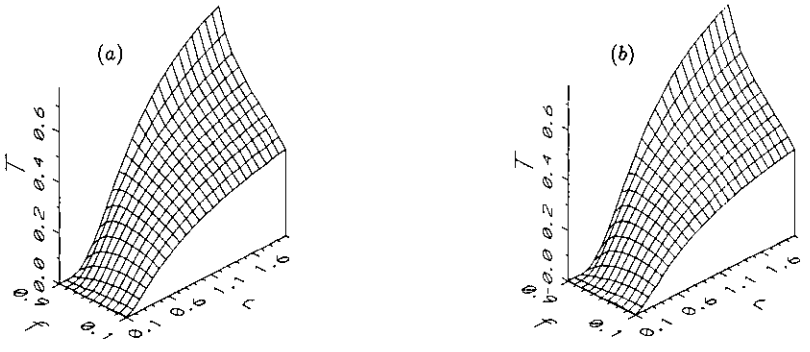

Figure 1. Transmittance as a function of f and r: (a) classical; (b) quantum. The surfaces have been constructed from 625 points in the f-r plane.

0305-4470/91/092003+10$03.50

2. Comparison between classical and quantum transmittances

We shall use, to fix ideas and make comparisons with some analytical results, a particular potential in a series of calculations

$$V = V_0/\cosh^2(ax). \tag{1}$$

However, our treatment can be applied quite generally to any potential by determining its characteristic length $1/a$, and its maximum value V_0, as shown below. Unless stated otherwise V_0 will be considered positive.

It is convenient to write the time-dependent Schrödinger equation in a dimensionless form:

$$\mathrm{i}\partial\Psi/\partial\tau = -\partial^2\Psi/\partial z^2 + U\Psi \tag{2}$$

$$\tau = (t\hbar a^2)/(2m) \qquad z = xa \qquad U = (2mV)/(\hbar^2 a^2) \tag{3}$$

where τ, z and U, the dimensionless time, position and potential, have been expressed in terms of $\hbar = h/2\pi$, m (the mass), and the corresponding dimensional quantities t, x and V. The dimensionless potential strength parameter (height of the barrier in dimensionless energy units) is defined as $U_0 = 2mV_0/(a^2\hbar^2)$. The initial Gaussian wavefunction at $t = 0$,

$$\psi = [2\pi\delta^2]^{-1/4} \exp[-(x-x_0)^2/(4\delta^2)] \exp[\mathrm{i}p_0(x - x_0/2)]$$

can also be made dimensionless by multiplying by $a^{-1/2}$. At $\tau = 0$, and using (3) it is given by

$$\Psi = [2\pi\Delta^2]^{-1/4} \exp[-(z-z_0)/(4\Delta^2)] \exp[\mathrm{i}P_0(z - z_0/2)]$$

where z_0 is the centre of the packet, $\Delta^2 = a^2\delta^2$ is the dimensionless second moment (variance) of $\Psi(z)\Psi(z)^*$ in coordinate space, and $P_0 = p_0/(a\hbar)$ is the dimensionless initial average momentum. By Fourier transformation we obtain

$$\Psi(P)\Psi(P)^* = [2\pi\sigma^2]^{-1/2} \exp[-(P-P_0)^2/(2\sigma^2)] = \mathscr{Z}[(P-P_0)/\sigma] \tag{4}$$

where $\sigma^2 = 1/(4\Delta^2)$ is the dimensionless variance in momentum space, and $\mathscr{Z}$ is the symbol to denote a Gaussian (normal) distribution. The dimensionless energy of the initial packet can be decomposed into a 'pseudo-kinetic energy' term, which corresponds to the kinetic energy of a classical particle with the average momentum of the packet, and a term due to the finite spread,

$$\varepsilon = 2m\langle E\rangle/(\hbar^2 a^2) = P_0^2 + \sigma^2 \tag{5}$$

where $\langle E\rangle$ is the dimensional average energy (note that ε is the true dimensionless kinetic energy in the asymptotic region). It is actually more convenient to characterize the initial wavefunction according to the variables f and r,

$$f = P_0^2/\varepsilon \qquad r = \varepsilon/U_0 \tag{6}$$

instead of using Δ and P_0. This is partly because the range of f goes from 0 to 1 and the range of interest for r goes from 0 to a few units, but also because of their physical content: r is the ratio between the energy of the packet and the potential barrier and f the fraction of energy in the form of 'pseudo-kinetic energy'. We shall next derive the classical transmittance formula. In terms of reduced quantities, and assuming that the classical quantum correspondence is established through the distribution of momenta (4), the fraction of classical particles that pass the barrier is given by

$$T = (2\pi\sigma^2)^{-1/2} \int_{U_0^{1/2}}^{\infty} \exp[-(P-P_0)^2/(2\sigma^2)]\,\mathrm{d}P. \tag{7}$$

By means of the change of variable $\Pi = P/U_0^{1/2}$ one obtains:

$$T = [2\pi(1-f)r]^{-1/2} \int_1^\infty \exp\{-[\Pi - (fr)^{1/2}]^2/[2r(1-f)]\}\, d\Pi$$

$$= 1 - \mathcal{P}[(1-M)/S]. \tag{8}$$

$\mathcal{P}[(1-M)/S]$ is the probability integral of the Gaussian distribution $\mathcal{Z}[(\Pi - M)/S]$, where $M = (fr)^{1/2}$ is the mean and $S^2 = [(1-f)r]$ the variance. Equation (8) is our central result. Note that the only required assumption to arrive at this expression is that the classical ensemble associated to the quantum state has the marginal distribution (4). This leaves the ensemble undetermined, but we do not need to be more specific for our purpose. Anyway, for more general applications, a Wigner distribution could be used to determine the weights.

The form (8) is better than (7) because we have reduced the number of relevant variables to two, namely, f and r. Note in particular that once these variables are fixed, the classical transmittance is independent of the value of the strength constant U_0 (except for the $U_0 = 0$ case; see below). It is also independent of the initial position of the packet, z_0, which means that the width of the spreading packet in coordinate space at the collision is irrelevant, the only quantity of importance being the minimum value Δ at $\tau = 0$. Another interesting 'prediction' of (8) is that the transmittance is independent of the particular shape of the potential.

Unfortunately, the quantum counterpart of (8) is not analytical in general and has to be evaluated by numerically solving the time-dependent Schrödinger equation. For this end we have used Koonin's method [1] (see the appendix). We shall *define* the quantum transmittance as the probability that the particle is at the right-hand side of the barrier at large positive times in the case that the incident packet approaches the barrier from the left

$$T = \lim_{\tau \to \infty} \int_0^\infty \Psi\Psi^*\, dz. \tag{9}$$

This definition is physically meaningful, and operationally more convenient than the standard one, 'the integral over all times of the particle flux observable evaluated at an asymptotic positive position (with positive momentum) divided by the number of incoming particles' [2]. Actually the two definitions lead in many cases to essentially the same numerical results. (The numerical agreement can be improved by dividing (9) by the probability of having positive momenta in the initial distribution (4). An expression in coordinate space for the standard definition of the transmittance in terms of a double integral can be found in [2].)

We have in figure 1(a) and 1(b) a comparison of the transmittances evaluated from (8) and (9) as a function of f and r for $U_0 = 10$. The agreement is excellent and several nuances of the quantum transmittance surface are perfectly (even with numerical accuracy) explained in classical terms. For instance, above threshold ($r > 1$) a large f value means that the classical distribution is peaked around P_0, allowing most of the particles to pass. At small f, P_0 is smaller and the distribution of momenta wider. As a consequence the transmittance decreases. Below threshold one can apply similar reasoning. For a peaked distribution (f close to one) it is more difficult to pass the barrier than for a wider one. This effect can however be compensated if f is large enough, because the average momentum grows with f, $P_0 = (frU_0)^{1/2}$. The result of these two opposite tendencies is the maximum below threshold of figure 1(a), accurately

reproduced in figure 1(*b*). We can actually determine the position of the maximum analytically by differentiating (8) with respect to f at fixed r. The maximum is given by the condition

$$\partial\mathscr{P}[(1-M)/S]/\partial f = \mathscr{Z}[(1-M)/S]\partial[(1-M)/S]/\partial f = 0$$

which after straightforward operations leads to $r = f$. Since $f \leqslant 1$, we can write:

$$f_{\max} = r \qquad (r \leqslant 1) \qquad\qquad f_{\max} = 1 \qquad (r > 1).$$

For the quantum calculations the initial packet has been located far enough from the potential to make the initial potential energy negligible. Once this condition is fulfilled the particular position has been found to be irrelevant, in agreement with the classical prediction, as far as the final value of the transmittance is concerned. (Checks have been done by varying z_0 (or equivalently τ_0) so as to change the width of the packet in coordinate space just prior to the collision by a factor of 100.) The detailed evolution and shape of the wavefunction depends, of course, on z_0, but we are not dealing with this issue here.

At this point it would seem that we can exactly reproduce the finest details of the quantum transmittance with the classical equation (8). However, the $f = 1$ limit is not represented in figure 1. Fortunately, this limit admits analytical examination. Physically it corresponds to stationary scattering, where the momentum distribution becomes a delta function. The quantum transmittance is given by [3]

$$T = \sinh^2(\pi P)/\{\sinh^2(\pi P) + \cos^2[\pi(1-4U_0)^{1/2}/2]\} \qquad 4U_0 < 1 \tag{10a}$$

$$T = \sinh^2(\pi P)/\{\sinh^2(\pi P) + \cosh^2[\pi(4U_0-1)^{1/2}/2]\} \qquad 4U_0 > 1 \tag{10b}$$

while, since the limit of the classical Gaussian $\mathscr{Z}[(\Pi - M)/S]$ as $f \to 1$ is a delta function, the classical transmittance is at this limit:

$$\begin{aligned} &T_{\mathrm{cl}} = \int_1^\infty \delta(\Pi - r^{1/2})\, \mathrm{d}\Pi \\ &T_{\mathrm{cl}} = 0 \qquad r < 1 \qquad\qquad T_{\mathrm{cl}} = 1 \qquad r > 1. \end{aligned} \tag{11}$$

This transmittance, which is standardly considered as the 'classical' one, is in clear contrast with the quantum results. However one should note that the quantum transmittance approaches the step behaviour at large positive U_0. To be exact, the limit of (10*b*) is

$$T \xrightarrow[\text{large } U_0]{} [1 + \mathrm{sgn}(r-1)]/2$$

where sgn is the sign distribution.

The existence in general of a difference between (10) and (11) is the result of an exclusive quantum behaviour not described in the classical equation, namely, the dependence with respect to the parameter U_0 in addition to the parameters r and f. To check the importance of this effect we have performed sweeps of U_0 summarized in figure 2 for fixed r and f. The general trend in the studied interval is a reduction of the classical quantum disagreement with increasing U_0. By the scaling of (3), U_0^{-1} is a measure of how quantum the system is, and the large U_0 limit is essentially a semiclassical limit. The origin of the low U_0 quantum behaviour is the fact that as U_0 tends to zero the quantum transmittance tends to one, disregarding a possible contribution to the initial packet of negative momenta, or dividing T by the probability of

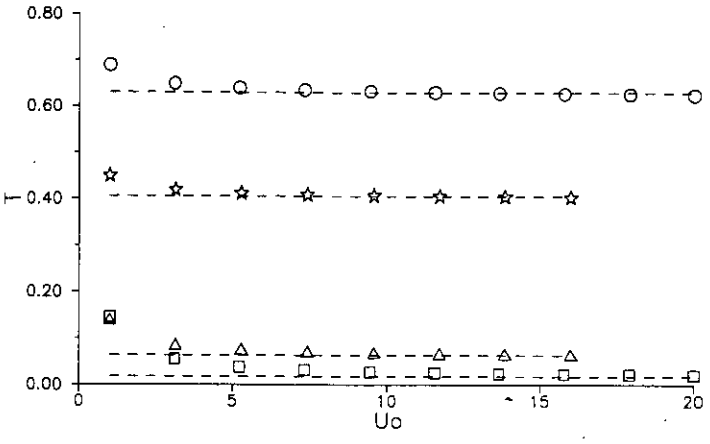

Figure 2. Transmittance against U_0 for (*a*) $r=1.8$; $f=0.8$ (circles); (*b*) $r=1.8$, $f=0.3$ (stars); (*c*) $r=0.3$, $f=0.8$ (triangles); (*d*) $r=0.3$, $f=0.3$ (squares). The broken lines correspond to the classical values obtained via (8) with the values for r and f given in (*a*)-(*d*).

having initial positive momenta. Nevertheless, $U_0=0$ is classically a singular point where (8) cannot be applied (note that the definition of Π before (8) involves $U_0^{1/2}$ in the denominator). Using the original equation (7) we recover, under the same positive momentum assumption used in the quantum case, $T=1$ for $U_0=0$. This classical discontinuity does not arise in quantum mechanics, where the $U_0=0$ limit and the large U_0 limit are smoothly joined.

The above considerations apply quite generally to any positive semidefinite potential. Note however that the occurrence of wells (regions with $U<0$) introduces in principle an additional source of quantum classical disagreement since they can reflect part of the quantum wavepacket but do not affect the classical passage. In particular, if a well potential is considered rather than a barrier ($U\leqslant 0$ at all z) the quantum transmittances are not reproduced classically. The reflection effect can be important for the square well but tends to be of less importance for smooth potentials.

In fact the possible influence of wells is but a particular case of a more general 'variable' affecting the quantum results that does not arise in the classical formula (7), the shape of the potential. To check the effect of different potential shapes we have calculated the transmittance curve for $f=0.7$ and $U_0=10$ for five different potentials. In addition to (1) we have used a Gaussian V_g, a square barrier V_b, a Lorentzian V_l, and a double barrier V_d:

$$\begin{aligned} &V_g = V_0 \exp(-x^2a^2) \\ &V_b = V_0 \quad |x|\leqslant 1/a \qquad V_b = 0 \quad |x|>1/a \\ &V_l = (a^{-2}V_0)/(a^{-2}+x^2) \\ &V_d = V_0(ax/2)^2 \exp[a(2/a-|x|)]. \end{aligned} \tag{12}$$

The results for V, V_g, V_l and V_d are very close to one another, and almost coincident with the classical prediction (figure 3), but the square barrier yields differences (at $f=0.7$ we have performed a second calculation by increasing U_0 by a factor of two for V_b without significantly changing the results of figure 3), which can also be found in the $f\to 1$ mono-energetic limit by comparing (11) with the analytical expression for

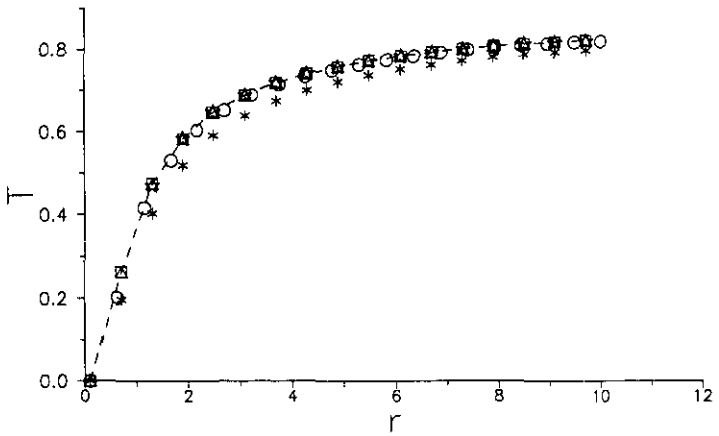

Figure 3. *Transmittance against r at $f=0.7$ for the potentials V (squares), V_g (triangles), V_l (stars), V_b (asterisks) and V_d (circles) (see (12) for the definitions). The broken line is the classical calculation.*

the transmittance of the square barrier (see, e.g., [3]). The difference at $f=1$ does not disappear at large U_0 in this case.

We should not be surprised by the disagreement with the classical transmittance for the square barrier since the differential equations of classical motion are singular (classical trajectories can however be defined for discontinuous potentials with the aid of variational formulation such as the least action principle).

One important potential source of differences between the classical and the quantum transmittances is the existence of resonances. For example, it has been found that the transmittance curves for separable potentials (in the stationary limit) show interesting and very different shapes from the classical transmittances [4, 5]. In this case however the classical quantum comparison for wavepackets is not trivial since the classical counterpart of the separable potential should consider momentum dependent forces. The square barrier is another case where multiple transmittance resonances are present.

For illustrative purposes we have chosen the double barrier V_d, since a nice isolated resonance can be studied (figure 4). This potential has been used for resonance analysis. in the context of s-wave scattering [6]. In our application the boundary conditions imposed on the wavefunction are different and correspond to one-dimensional scattering. Figure 4 shows a transmittance resonance peak slightly below the classical threshold in the stationary limit (peaked full line). The curve has been obtained by numerically solving the stationary Schrödinger equation at small energy intervals. (See the appendix for details). For $f=0.9999$ (triangles) the transmittance of the time-dependent wavepacket still keeps the resonance features. The classical result is of course very different (broken line). At $f=0.99$ however the resonance can no longer be recognized and the classical results are closer to the quantum ones. At $f=0.7$ classical and quantum results are in good agreement. This kind of behaviour can be expected in general, the details of the smoothing of the resonance depending on the relative widths of the resonance peak and of the time-dependent packet. In our example, with $U_0=5.41$, the half width at half height of the resonance peak is roughly 0.13 dimensionless energy units, equivalent to $(\Gamma/2)_{res}\approx 0.3$ dimensionless momentum units. Using (5) and (6) one finds that for $f=0.9999$, $(\Gamma/2)_{Gaussian}\approx 0.03 \ll \Gamma/2$ while for $f=0.7$, $(\Gamma/2)_{Gaussian}\approx 1.4 \gg (\Gamma/2)_{res}$. In the case $f=0.99$, $(\Gamma/2)_{Gaussian}$ and $(\Gamma/2)_{res}$ are similar.

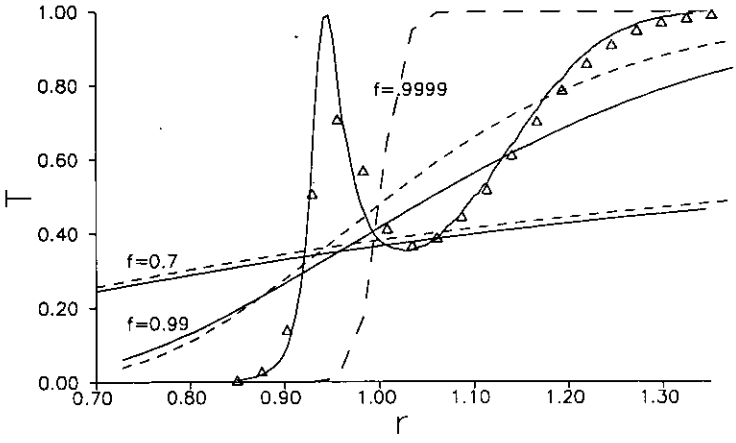

Figure 4. Transmittance against r at different f values for V_d ($m = a = h = l$, $V_0 = 2.7067$, ($U = 5.4134$)). The peaked full line is the transmittance in the stationary limit (the corresponding classical result is a sharp step at $r = 1$). The triangles are the quantum results for $f = 0.9999$. The broken lines are the classical predictions, and the full lines are the quantum calculations.

In summary, the classical transmittance can be an excellent approximation for the quantum one regardless of the potential shape, provided that the potential is smooth and the parameter U_0 is large enough. A remarkable exception is the occurrence of quantum resonance bumps that cannot be reproduced classically. However, when considering wavepackets with non-zero width in momentum space ($f \neq 1$), of the order of the resonance width or larger, the resonances of the mono-energetic limit are smoothed out (see figure 4), so even when the potential admits resonances the classical transmittance can be in close agreement with the quantum one.

3. Conclusions and discussion

A classical formula for the transmittance through a potential barrier has been shown to give very good agreement with the quantum results. The cases where this is not so have been discussed. The formula is based on the correspondence between a Gaussian wavefunction and a Gaussian classical distribution of particles, and yields the fraction of initial particles with energy higher than the barrier maximum. The formalism has been cast into dimensionless form to obtain reduced general laws depending on a few relevant dimensionless parameters.

A completely different approach to understand tunnelling classically, vividly described as 'classical high jumping', has been published recently [7]. The method is based on assigning a distribution of lengths to the classical bodies. It would be interesting to compare it with the present approach and see if a richer theory combining the two methods improves the classical results.

The following predictions of our classical formula have been contrasted (and confirmed except where stated) with quantum calculations.

(1) The transmittance does not essentially depend on the initial position of the packet (provided it is far enough from the potential, and the rest of the Gaussian parameters are fixed).

(2) The transmittance does not depend on the strength parameter U_0 for given f and r ratios (see text for definitions). This has been shown to be true in quantum mechanics for large enough U_0.

(3) The transmittance is independent of the potential shape. The exceptions are the discontinuous potentials, and potentials admitting resonances (when the width of the packet is lower than the resonance width).

(4) The above three statements can be summarized in one: the transmittance only depends on the ratios f and r. (Again, true for large enough U_0, and smooth potentials, with the possible exception of resonances in the mono-energetic limit.)

(5) The transmittance surface as a function of f and r has a maximum at $f = r$ (for $(f < 1)$ which can be understood in classical terms.

It is perhaps surprising that such an amount of detail on the transmittance can be derived from such a simple classical argument, especially as tunnelling is frequently considered one of the quintessential quantum phenomena. We believe that our study separates what is really quantum (resonance bumps, U_0 dependence, ...) from what is not (general features of the wavepacket transmittance) and points out that the classical quantum correspondence is better implemented at the level of phase-space distributions, where some of the 'quantum' effects admit a purely classical visualization. At this point we could distinguish between two different types of tunnelling: if the passage of the barrier when the expectation value of the energy is below threshold can be reproduced classically, we have 'classical ensemble tunnelling'. The opposite case corresponds to 'quantum tunnelling'. Thus, resonance tunnelling, or the tunnelling in the stationary limit, are purely quantum. It is interesting to notice however that, for the negative harmonic barrier, a classical explanation exists for the tunnelling in the stationary limit making use of the Wigner formalism. It is known that for quadratic potentials the evolution of the Wigner function is purely classical. Tunnelling is then due to the possibility of having 'wrong energies' in the Wigner distribution associated to the stationary scattering state [8].

From a practical point of view, the quantitative accuracy obtained classically and the simplicity of the approach warrants applications of the method in any physical situation where tunnelling has to be considered [9]. We have compared our classical

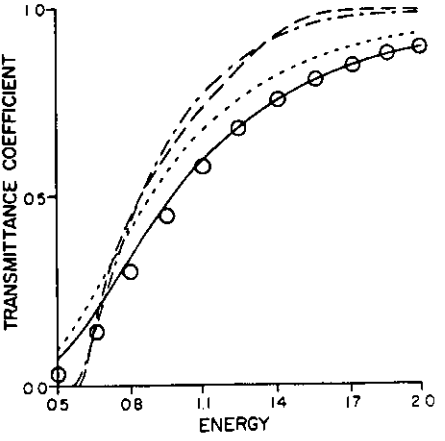

Figure 5. Transmittance against 'energy' $= r/1.05$ at $f = 1/1.05$, taken from [2] for V_2. The full line is the exact quantum result while the broken, dotted, and chain lines are different semiclassical approximations. The circles are obtained from the classical formula (8).

transmittance with various semiclassical methods used in [2] and the exact results, see figure 5. The classical formula (8) has the best performance and it is the easiest to implement. The classical transmittance should serve then as a reference test for semiclassical methods, and a starting point for further quantum corrections. For some applications, it will be necessary to obtain classical approximations for the wavefunction, i.e. trajectories should be run with the members of the classical ensemble. For two or more dimensions this will be necessary in general even for calculating the transmittance due to the coupling between the different degrees of freedom.

In summary, the 'quantum' passage through a barrier, including tunnelling, admits a classical qualitative and quantitative counterpart in terms of classical phase-space ensembles, which accurately reproduces the quantum transmittance, except in the following cases: in the stationary limit, for low U_0, for discontinuous potentials, and when resonance widths are larger than the packet width.

Acknowledgments

I acknowledge R F Snider for useful comments on the original. R F Snider and R E Turner provided a code and information on Koonin's method. Discussions with R D Levine and R B Gerber are also acknowledged. The work has been partly supported by Spanish Ministerio de Educación y Ciencia.

Appendix

In this appendix we provide some details on the quantum calculations. Koonin's method [1] of solving the time-dependent Schrödinger equation is based on a discretization of position and time. For most of the calculations we have used a position step of 0.12, a time step $\simeq U_0$, and 2400 spatial points. The 'infinite time' required for obtaining the transmittance is actually taken as the time when the transmittance (which is computed at a given time interval) remains stationary. This condition cannot be fulfilled in the cases where the packet becomes too broad in coordinate space or when it moves too fast because the boundary effects of the enclosing box cannot be neglected. For additional information on this point see [10].

The solution of the stationary Schrödinger equation has been carried out by converting first this second-order differential equation into two coupled first-order differential equations for $x = \Psi$ and $y = \partial\Psi/\partial z$. The system is then decomposed into four coupled real equations and solved with a library subroutine (IMSL's DGEAR). The initial conditions are chosen according to the outgoing boundary condition of the scattering function with unit outgoing density, and the 'trajectories' determining x and y are run 'backwards', i.e. from right to left (this amounts to considering Ψ^* rather than Ψ, since the outgoing momentum is reversed). The transmittance can then be easily obtained from the asymptotic form on the left. As far as we know this procedure is described here for the first time.

References

[1] Koonin S E 1985 *Computational Physics* (Menlo Park: Benjamin)
[2] Turner R E and Snider R F 1987 *J. Chem. Phys.* **87** 910

[3] Landau L D and Lifshitz E M 1958 *Quantum Mechanics* (Reading, MA: Addison-Wesley)
[4] Muga J G and Snider R F 1990 *Can. J. Phys.* **68** 403
[5] Hammerich A D, Muga J G and Kossloff R 1989 *Isr. J. Chem.* **29** 461
[6] Maier C H, Cederbaum L S and Domcke, W 1980 *J. Phys. B: At. Mol. Phys.* **13** L119
[7] Cohn A and Rabinowitz M 1990 *Int. J. Theor. Phys.* **29** 215
[8] Balazs N L and Voros A 1990 *Ann. Phys., NY* **199** 123
[9] Hauge E H and Stovneng J A 1989 *Rev. Mod. Phys.* **61** 917
[10] Goldberg A, Schey H M and Schwartz J L 1967 *Am. J. Phys.* **35** 177